Available online at www.sciencedirect.com
SCIENCE DIRECT®
International Journal of Thermal Sciences 45 (2006) 1021–1026
International Journal of Thermal Sciences
www.elsevier.com/locate/ijts

A numerical study of channel-to-channel flow cross-over through the gas diffusion layer in a PEM-fuel-cell flow system using a serpentine channel with a trapezoidal cross-sectional shape ☆

Lan Sun [a], Patrick H. Oosthuizen [a,*], Kim B. McAuley [b]

[a] *Department of Mechanical and Materials Engineering, McLaughlin Hall, Queen's University, Kingston, ON, Canada K7L 3N6*
[b] *Department of Chemical Engineering, Dupuis Hall, Queen's University, Kingston, ON, Canada K7L 3N6*

Received 30 August 2005; accepted 10 January 2006

Available online 20 February 2006

Abstract

A numerical study of pressure distribution and flow cross-over through the gas diffusion layer (GDL) in a PEMFC flow plate using a serpentine channel system has been undertaken for the case where the channel has a trapezoidal cross-sectional shape. The flow has been assumed to be 3-D, steady, incompressible and single-phase. The flow through the porous diffusion layer has been described using the Darcy model. The governing equations have been written in dimensionless form and solved by using the commercial CFD solver, *FIDAP*. The results obtained indicate that: (1) the size ratio, R, of trapezoidal cross-sectional shape has a significant effect on the flow cross-over. As R increases, the flow cross-over through GDL increases; (2) the ratio R also has a significant effect on the pressure variation in the flow field for both cross-over and no cross-over cases; (3) flow cross-over has a significant influence on the pressure variation through the channel, tending to decrease the pressure drop across the channel; (4) an increase in Re number can lead to a slight increase in the flow cross-over.

Keywords: PEM fuel cell; Numerical model; Fluid flow; Flow plate; Pressure drop; Gas diffusion layer; Flow cross-over; Trapezoidal cross-section; Serpentine channel; Permeability

1. Introduction

On the cathode side of a PEM fuel cell, the air usually flows through serpentine channels with a square cross-section in a flow plate. There is a porous diffusion layer adjacent to the flow plate. Flow cross-over of air through the porous diffusion layer from one part of the channel to another can occur. This cross-over, as shown in Fig. 1, is a result of the pressure differences between different parts of the channel, and it causes the flow rate through the channel to vary with the distance along the channel. Since one of the important functions of the flow plate (with the serpentine channel) is to supply the fuel and air for the electrochemical reaction, the performance of a PEM fuel cell is strongly dependent on the transport processes occurring within the flow fields. The geometry of flow plate has a significant effect on the nature of the fluid flow, heat and mass transfer and so has an influence on the performance of the fuel cell. The purpose of the present work is to provide some basic information on the effects of channel cross-section shape on the flow field for the particular case where the channel cross-section is trapezoidal. Flow in a particular serpentine channel system, which is representative of that used in PEMFC flow plates, has been considered. The emphasis of this work is on the effect of the channel shape on the pressure distribution and channel-to-channel flow cross-over through the gas diffusion layer (GDL). The trapezoidal shape of the channel cross-section may be beneficial for reducing the pressure drop and for improving overall fuel cell performance. Augmenting flow cross-over through GDL will lead to higher oxygen concentrations at the surface of the cathode catalyst layer under the GDL, which, in turn, leads

☆ A preliminary version of this paper was presented at ICMM05: Third International Conference on Microchannels and Minichannels, held at University of Toronto, June 13–15, 2005, organized by S.G. Kandikar and M. Kawaji, CD-ROM Proceedings, ISBN: 0-7918-3758-0, ASME, New York.

* Corresponding author. Tel.: +1 613 533 2573; fax: +1 613 533 6489.
E-mail address: oosthuiz@me.queensu.ca (P.H. Oosthuizen).

1290-0729/$ – see front matter © 2006 Elsevier SAS. All rights reserved.
doi:10.1016/j.ijthermalsci.2006.01.005

Nomenclature

A_c	cross-sectional area of channel
A	the length of the narrow side of the trapezoidal cross-section
B	the length of the wide side of the trapezoidal cross-section
CFD	computational fluid dynamics
d_H	hydraulic diameter of the trapezoidal cross-section
D_H	dimensionless hydraulic diameter of the trapezoidal cross-section, $= d_H / W_c$
f	Darcy friction factor
F	dimensionless flow rate at any specified section of the channel, see Eq. (3)
F_{inlet}	dimensionless flow rate at inlet section of the channel
$F_{\min}$	minimum dimensionless flow rate in channel
ΔF	maximum difference between the dimensionless flow rate at the inlet and the minimum dimensionless flow rate in the channel, see Eq. (4)
FC	fuel cell
GDL	gas diffusion layer
H	height of the channel
K	permeability of gas diffusion layer
K_P	dimensionless permeability of gas diffusion layer, $= K / W_C^2$
MEA	membrane electrode assembly
p	pressure
p_{out}	pressure at the channel outlet
P	dimensionless pressure, see Eq. (5)
ΔP	the overall dimensionless pressure drop between the channel inlet and outlet
P_{inlet}	dimensionless pressure at the channel inlet
P_{outlet}	dimensionless pressure at the channel outlet
P_c	perimeter of the trapezoidal cross-section
PEM	polymer electrolyte membrane
R	ratio of the length of the wide side of the trapezoidal channel to the length of the narrow side of the trapezoidal channel, $= B/A$
Re	Reynolds number based on the average width of the channel
Re_D	Reynolds number based on the hydraulic diameter of the trapezoidal cross-section
t	GDL thickness
U_c	mean velocity at any specified section of the channel
U_m	mean velocity at inlet section of the channel
W	land width
W_c	average width of the channel
W_m	the center line distance of the adjacent channels
ρ	density

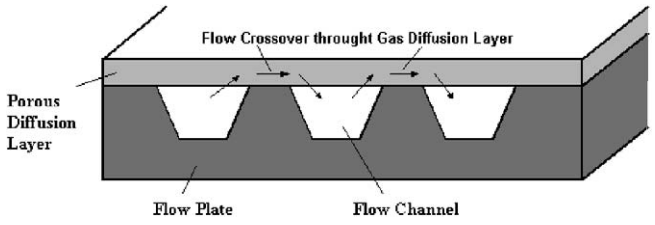

Fig. 1. Flow situation considered in present study.

to higher electrochemical reaction rates, see Sun et al. [11]. The situation considered in the present study is as shown in Fig. 1. Since this work only deals with the basic flow and does not consider heat and mass transfer, the assumed boundary condition on the top surface at the interface between the GDL and the catalyst layer is simply that the velocity component normal to the surface is zero. The present study is intended to help to get a better understanding for some of the factors that influence the design of the bipolar plates in PEM fuel cells.

By taking advantage of developments in CFD software and computational hardware, recent PEMFC modeling has been able to include all the cell components, including the gas channels and the porous diffusion layer. The detailed study of the convective and diffusive flow in the flow field is thus now possible. Typical papers concerned with this type of modeling are those of Dutta and Shimpalee [3], Berning [1], Yuan, Rokni and Sunden [15,16]. However, all of the models mentioned above have dealt with a straight channel in the flow plate. In an attempt to extend this numerical work to deal with more realistic flow plate geometries, Yi and Nguyen [13] used a two-dimensional model of multi-component transport in the porous electrodes to study flow with an interdigitated gas distributor. Later, He et al. [4] developed a detailed two-phase model using the same flow plate design. Driven by an interest in serpentine-channel flow systems, Dutta and Shimpalee [2] studied a 3-D PEMFC flow field with serpentine channels. Their results indicated that flow distributions in both anode and cathode channels were significantly affected by the mass consumption patterns on the membrane electrode assembly (MEA). Also, water transport was governed by both electro-osmosis and diffusion processes. They also found that the flow through the porous gas diffusion layer was significant, and that the overall pressure drop was lower than that expected by considering just the flow in a serpentine channel. However, they did not study in detail the factors that influence these pressure drops and the flow cross-over through the GDL. The pressure differences across the flow plate can be influenced by flow cross-over through the GDL for different flow plate geometries and configurations. Oosthuizen et al. [6] studied the pressure and temperature distribution in PEMFC flow plates with a single serpentine channel system having a square cross-section. They concluded that channel-to-channel flow cross-over through the GDL is only significant when the permeability exceeds approximately 1.0E–11 m^2. Oosthuizen et al. [7] also studied the effect of the land width in a square cross-sectional channel system on the fluid flow.

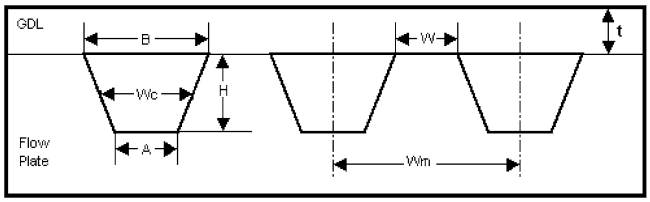

Fig. 2. Geometry of the trapezoidal cross-sectional channel.

Several studies of the flow characteristics in situations involving channels with different cross-sectional shapes have been undertaken, e.g., see Yuan et al. [14], Kumar and Reddy [5] and Oosthuizen [8]. Other papers related to the effect of trapezoidal channel cross-section on microchannel flows are those of Wu et al. [12] and Qu et al. [9,10]. Available studies indicate that channel cross-sectional shape and flow cross-over have a significant influence on the flow field, but no general conclusions regarding this influence have been developed. Therefore, the importance of the channel-to-channel flow cross-over in determining the flow rates in different parts of the channel, and the pressure variation along the channel has been numerically examined in the present study for the case where the channel has a trapezoidal cross-sectional shape. No studies of flow cross-over in situations involving trapezoidal channels appear to be available.

A single 3-pass serpentine-channel flow plate with trapezoidal cross-sectional shape has been considered here. The height of the channel H is equal to the average channel width W_c, as shown in Fig. 2. The distance between adjacent channels W_m is fixed. The land width W is equal to the length of the narrow side of the trapezoidal channel, A. The thickness of GDL, t, is shown on the upper corner of the right side of the figure. The length of the straight portions of the channels is 20 times the average channel width.

2. Solution procedure

It has been assumed that:

- the flow is 3-D, steady and single-phase;
- gas properties are constant;
- the flow through the porous diffusion layer can be described using the Darcy model;
- the velocity is uniform over the channel inlet plane;
- the normal velocity components are zero on all surfaces of the GDL, except at the interface between the gas diffusion layer and flow channels.

The governing equations have been written in dimensionless form using the average channel width, W_c, as the length scale and the mean velocity in the channel inlet, U_m, as the velocity scale. The solution parameters in the resultant set of dimensionless equations are:

- Reynolds number (based on the average channel width, W_c, and on the mean velocity at the channel inlet, U_m). Results are discussed for $Re = 50$, 100 and 200;

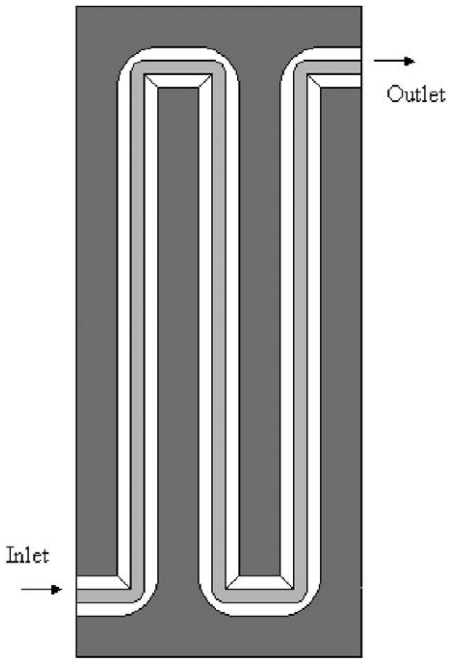

Fig. 3. Single 3-pass serpentine channel with trapezoidal cross-section.

- Dimensionless permeability of the gas diffusion layer. Results for values of $K_P = 1.0\text{E}{-13}$ (the no cross-over case) and $K_P = 1.0\text{E}{-4}$ (the cross-over case) are discussed. Note that the dimensionless GDL permeability, K_P, is related to the actual permeability K by

$$K_P = K / W_c^2 \tag{1}$$

- Dimensionless GDL thickness (the thickness of gas diffusion layer, t, relative to the average channel width, W_c). Results are presented for a value of 0.25;
- Dimensionless channel shape (the ratio, R, of the length of the wide side of the channel, B (see Fig. 2) to the length of the narrow side of the channel, A, for the trapezoidal cross-section shape):

$$R = B/A \tag{2}$$

Values between 1 and 7 are considered;

- Flow plate geometry. Attention is restricted to a flow plate having a single 3-pass serpentine channel, as shown in Fig. 3.

The solution was obtained by simultaneously solving for the flow velocity and pressure distributions in the channel and in the gas diffusion layer. The simulation was carried out using the commercial finite element method software package *FIDAP* v. 8.7.2. Results were obtained for a given situation with various numbers of grid-points and various values of the convergence-criterion. These indicate that the results presented here are grid-point number and convergence-criterion independent to better than one percent.

3. Results

Attention is first given to examining variations in the dimensionless flow rate along the channel (neglecting oxygen consumption or water generation by electrochemical reactions). Changes in this flow rate give a direct indication of the magnitude of the flow cross-over. The amount of variation in the flow rate along the channel depends on the pressure distribution. The dimensionless mass flow rate is defined as:

$$F = \frac{U_c A_c}{U_m W_c^2} \tag{3}$$

where F is the dimensionless flow rate perpendicular to the channel cross-section, U_c is the mean velocity of this cross-section and A_c is the area of this cross-section. Note that A_c does not depend on the dimensionless channel shape parameter, R.

Typical variations of dimensionless flow rate within the channel with distance along the channel for various values of the channel size ratio, R, for $Re = 100$ are shown in Fig. 4. Gas that does not flow within the channel is, of course, flowing through the GDL. Dimensionless flow rates that are significantly below 1 indicate that there is substantial flow cross-over. The results given in Fig. 4 indicate that there is significant cross-over for a dimensionless permeability of 1.0E–4, but negligible cross-over for a dimensionless permeability of 1.0E–13. It can be seen that there is a large flow out of the first pass of the channel, across the GDL. All of the gas that flows out the channels eventually flows back into the channel in the final pass, so that the dimensionless flow rate at the outlet is 1. The fraction of the total flow that remains within the channel is lowest in the middle pass.

It can be seen from the results given in Fig. 4 that the ratio R has a significant effect on the flow rate along channel for a dimensionless permeability, 1.0E–4, i.e., for the flow cross-over case. With an increase in the ratio R, the flow cross-over increases. As R increases, the wider side of the trapezoidal shape gets bigger and the land width gets smaller, tending to promote the flow through the GDL. This tendency is further illustrated by the results shown in Fig. 5, which shows how ΔF, the maximum difference between the local dimensionless flow rate in the channel and that at the inlet,

$$\Delta F = \frac{F_{\text{inlet}} - F_{\min}}{F_{\text{inlet}}} \tag{4}$$

changes with channel shape and Re number. When Re number increases, the flow cross-over increases slightly. However, the effect of Re on the cross-over with a given channel cross-sectional shape is small.

Next, we examine pressure variation along the channel. The dimensionless pressure is expressed relative to the exit plane pressure as follows:

$$P = \frac{p - p_{\text{out}}}{\rho U_m^2} \tag{5}$$

Typical variations of dimensionless pressure along the centerline of the channel at $Re = 50$ are shown in Fig. 6. The total channel length of single 3-pass channel is 67 average channel widths. Results for both the no cross-over and cross-over cases are given. Fig. 6 reveals that flow cross-over has a significant effect on the channel pressure variation. The overall pressure drop between the inlet and outlet decreases (for a particular R value) when cross-over is present. Pressure drop is also affected by the ratio R for both of the cross-over and the no cross-over cases. As the R value increases, for the no cross-over case, the pressure drop increases slightly, but for the cross-over case, the

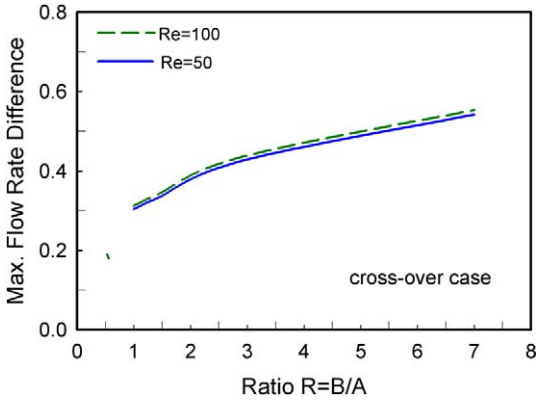

Fig. 5. Variation of maximum flow rate difference with the ratio R values for cross-over case.

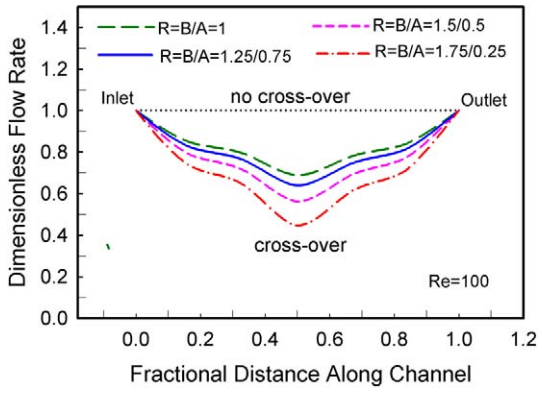

Fig. 4. Variation of dimensionless flow rate with distance along channel for different ratio R values, $Re = 100$.

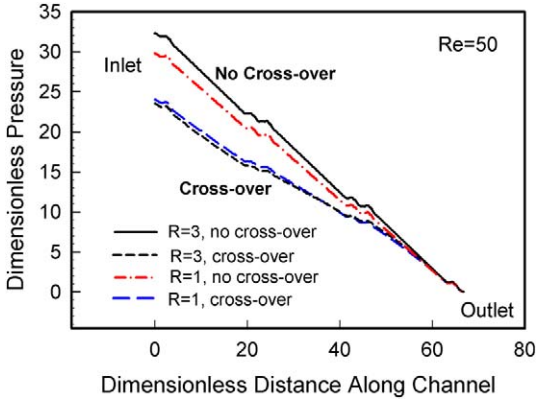

Fig. 6. Variation of dimensionless pressure along channel for different ratio R values, $Re = 50$.

pressure drop decreases slightly. Similar results were obtained at $Re = 100$, as shown in Fig. 7.

The effect of channel geometry on the overall dimensionless pressure drop between the inlet and outlet, i.e.,

$$\Delta P = P_{\text{inlet}} - P_{\text{outlet}} \tag{6}$$

is further examined in Fig. 8. It was found that, in all cases, an increase in the ratio R resulted in an increase in the overall dimensionless pressure drop for the no cross-over case and in a decrease in the dimensionless pressure drop for the cross-over case.

Typical pressure variations along the straight sections of the 3 channel passes are shown in Fig. 9, for $Re = 200$ and $R = 3$. In fully developed channel flow without cross-over, the pressure gradient should be constant along a straight section of channel. Therefore, Fig. 9 indicates that, at the Reynolds number considered in this study, the flow almost reaches a fully developed state near the middle of the first channel pass. However, some small effects of the entrance and of the bends at the ends of the passes are apparent.

The pressure gradient in fully developed channel flow is usually expressed in terms of the friction factor, f. Here, the Darcy formulation is used:

$$-\frac{\mathrm{d}p}{\mathrm{d}x} = f\frac{\rho u_m^2}{2d_H} \tag{7}$$

where d_H is the hydraulic diameter defined by,

$$d_H = \frac{4 \times \text{cross-sectional area}}{\text{wetted perimeter}} = \frac{4A_c}{P_c} \tag{8}$$

The friction factor equation can be written in terms of the dimensionless variables as,

$$-\frac{\mathrm{d}P}{\mathrm{d}X} = \frac{f}{2D_H} \tag{9}$$

where D_H is the dimensionless hydraulic diameter given by,

$$D_H = \frac{4A_c}{P_c W_c} = \frac{d_H}{W_c} \tag{10}$$

In fully developed laminar flow, it is usually adequate to assume that,

$$f = \frac{K'}{Re_D} \quad \text{i.e.,} \quad f\,Re_D = K' \tag{11}$$

where K' is a constant and Re_D is the Reynolds number based on the hydraulic diameter. Since Re in this study is defined using the average channel length, W_c, as length scale, it follows that,

$$f\,Re_D = -2Re\frac{\mathrm{d}P}{\mathrm{d}X}D_H^2 \tag{12}$$

The $f\,Re_D$ values can be obtained from the pressure variation along the middle portion of the straight section of the first pass

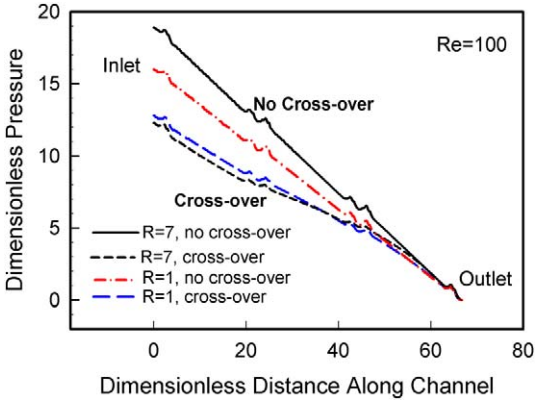

Fig. 7. Variation of dimensionless pressure along channel for different ratio R values, $Re = 100$.

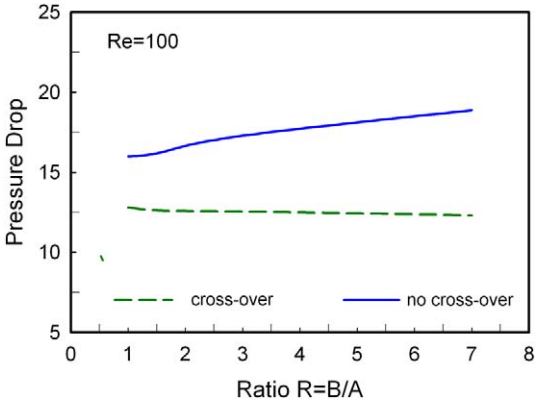

Fig. 8. Variation of dimensionless pressure drop between inlet and outlet of the channel with different R values for $Re = 100$.

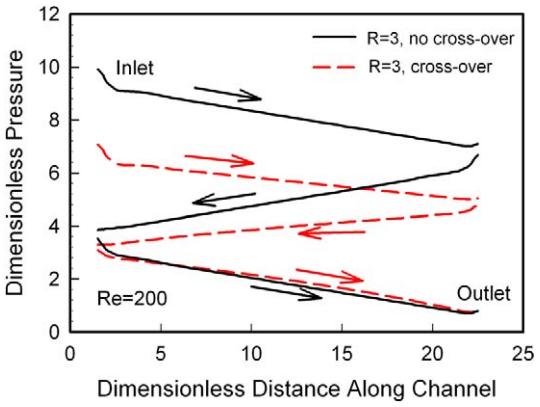

Fig. 9. Variation of dimensionless pressure along the straight sections of the 3-pass channel for $Re = 200$.

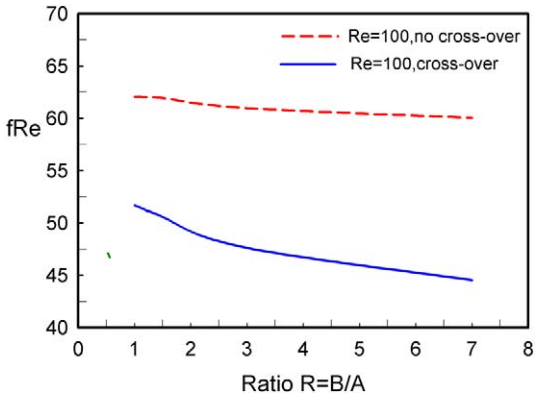

Fig. 10. Variations of $f\,Re_D$ with R values for both of cross-over and no cross-over cases, $Re = 100$.

for different channel cross-sectional shape ratios, R. Typical variations of $f\,Re_D$ with R for both the cross-over and no cross-over cases for $Re = 100$ are shown in Fig. 10, which shows that $f\,Re_D$ tends to a constant value of approximately 62 as R tends to 1 for the no cross-over case. However, $f\,Re_D$ is significantly decreased by the flow cross-over. Note that the $f\,Re_D$ value of 62, to which the no cross-over results tend as R tends to 1, is higher than the analytical value for fully developed laminar flow in a square channel (i.e. approximately 57) due to the presence of minor entrance and exit bend effects.

4. Conclusions

A 3-D numerical model of a PEM fuel cell flow field with single 3-pass serpentine channel was developed, and it provide valuable information about the pressure drop and flow cross-over through GDL. The results obtained by using the trapezoidal shape of the channel cross-section in present study indicate that,

- The trapezoidal cross-sectional shape ratio R has a significant effect on the flow cross-over. An increase in R is associated with an increase in the flow cross-over through GDL.
- The trapezoidal cross-sectional shape ratio R also has a significant effect on the pressure variation in the flow field for both the cross-over and the no cross-over cases.
- Flow cross-over has a significant influence on the pressure variation through the channel, tending to decrease the pressure drop across the channel.
- An increase in the value of Re is associated with a slight increase in the flow cross-over.

Acknowledgements

This work was supported by the Natural Sciences and Engineering Research Council of Canada and by E.I. du Pont of Canada.

References

[1] T. Berning, Three-dimensional computational analysis of transport phenomena in a PEM fuel cell, PhD dissertation, University of Victoria, Canada, 2002.

[2] S. Dutta, S. Shimpalee, J.W. Van Zee, Numerical prediction of mass-exchange between cathode and anode channels in a PEM fuel cells, Int. J. Heat Mass Transfer 44 (11) (2001) 2029–2042.

[3] S. Dutta, S. Shimpalee, J.W. Van Zee, Three-dimensional numerical simulation of straight channel PEM fuel cells, J. Appl. Electrochem. 30 (2000) 135–146.

[4] W. He, J.S. Yi, T.V. Nguyen, Two-phase flow model of the cathode of PEM fuel cells using interdigitated flow field, AIChE J. 46 (2000) 2053–2064.

[5] A. Kumar, R.G. Reddy, Effect of channel dimensions and shape in the flow field distributor on the performance of polymer electrolyte membrane fuel cells, J. Power Source 113 (2003) 11–18.

[6] P.H. Oosthuizen, L. Sun, K.B. McAuley, The effect of channel-to-channel gas crossover on the temperature and pressure distribution in PEM fuel cell flow plates, J. Appl. Thermal Engrg. 25 (2004) 1083–1096.

[7] P.H. Oosthuizen, L. Sun, K.B. McAuley, A numerical study of the effect of flow plate geometry on the pressure distribution and channel to channel flow cross-over in a PEM fuel cell using a serpentine flow channel system, in: Proceedings of IMECE'04, ASME International Mechanical Engineering Congress & Exposition, November 13–19, Anaheim, CA, USA, 2004.

[8] P.H. Oosthuizen, Flow and heat transfer in a simple trapezoidal minichannel flow system, in: Proceedings of 12th Annual Conference of the CFD Society of Canada, Heat Transfer II, May 9–12, Ottawa, Canada, 2004.

[9] W. Qu, G.M. Mala, D. Li, Heat transfer for water flow in trapezoidal silicon microchannels, Int. J. Heat Mass Transfer 43 (2000) 3925–3936.

[10] W. Qu, G.M. Mala, D. Li, Pressure-driven water flows in trapezoidal silicon microchannels, Int. J. Heat Mass Transfer 43 (2000) 353–364.

[11] W. Sun, B.A. Peppley, K. Karan, Modeling the influence of GDL and flow-field plate parameters on the reaction distribution in the PEMFC cathode catalyst layer, J. Power Sources 144 (2005) 42–53.

[12] H.Y. Wu, P. Cheng, Friction factors in smooth trapezoidal silicon microchannels with different aspect ratios, Int. J. Heat Mass Transfer 46 (2003) 2519–2525.

[13] J.S. Yi, T.V. Nguyen, Multi-component transport in porous electrodes of proton exchange membrane fuel cells using the interdigitated gas distributors, J. Electrochem. Soc. 146 (1) (1999) 38–45.

[14] J. Yuan, M. Rokni, B. Sunden, Simulation of fully developed laminar heat and mass transfer in fuel cell ducts with different cross-sections, Int. J. Heat Mass Transfer 44 (2001) 4047–4058.

[15] J. Yuan, M. Rokni, B. Sunden, Analysis of flow and heat transfer in PEM fuel cell ducts by an extended darcy model, in: Proceedings of the 13th International Symposium on Transport Phenomena, July 14–18, University of Victoria, Canada, 2002, pp. 838–842.

[16] J. Yuan, M. Rokni, B. Sunden, Modeling of two-phase flow in a cathode duct of PEM fuel cells, in: Proceedings of the 1st International Conference on Fuel Cell Science, Engineering and Technology, Rochester, NY, USA, 2003, pp. 463–470.